Thermoelectric properties of microstructures with four-probe versus two-probe setups

Glen D. Guttman, Eshel Ben-Jacob, and David J. Bergman
School of Physics and Astronomy, Raymond and Beverly Sackler Faculty of Exact Sciences, Tel-Aviv University, Ramat-Aviv 69978, Tel-Aviv, Israel
(Received 12 December 1995)

We study nonlocal thermoelectric transport properties of disordered mesoscopic systems in a four-probe setup. In particular, we vary the coupling of two of the probes to the sample. In the limit of weak coupling, we recover the two-probe thermoelectric transport coefficients. We find that the Onsager relations are satisfied in the disordered region. The effect of phase-incoherent transport on the two-probe conductance and thermopower is also studied in the limit of strong coupling of the probes. [S0163-1829(96)00920-4]

I. INTRODUCTION

The standard setup for the measurement of the transport coefficients of mesoscopic samples is a four-probe configuration. Therefore results of such experiments should be explained using a theoretical formalism suited for a four-probe setup. Indeed, Büttiker has resolved the controversy over the measured asymmetry of the magnetoconductance using a similar derivation.[1,2] A generalization, yielding the thermoelectric transport of a four-probe system, is presented in Ref. 3. In such systems nonlocal effects,[4] due to the phase coherence of electrons across the sample, are measurable. For example, a temperature drop between two contacts can induce a voltage drop between two different terminals, within the dephasing length L_ϕ.

When using a two-probe setup, in which the response of the system is measured between the same contacts through which the current is driven, one inevitably encounters a contact resistance. In these systems the conductance of a scattering barrier is given by the Landauer formula $G=(e^2/h)(t/r)$.[5] However, the total conductance, which includes the contact resistance,[6] is given by $G=(e^2/h)t$.[7] As noted in Ref. 8, it is only this total conductance that can be measured in a two-probe experimental setup. Several theoretical approaches have been utilized[9–11] in order to rederive the Landauer formula without including the contact resistances. In addition, two different approaches were used in order to generalize that formula and derive the thermoelectric coefficients of the mesoscopic region in a two-probe setup: one approach[12] assumes that a local thermodynamic affinity can be assigned to the mesoscopic region while the second approach[13] ascribes thermodynamic equilibrium properties only to the probes and assumes a generalized Ohmic response of the mesoscopic system to the affinities.

Here we derive the two-probe thermoelectric transport coefficients in a different way, by studying the specific four-probe configuration suggested in Ref. 9. Thus we avoid the contributions of the contacts to the transport and treat the mesoscopic region strictly by the laws of quantum mechanics. Equilibrium thermodynamic properties are ascribed only to probes connected to the sample. The same system is used to demonstrate the effect of phase-incoherent transport through the disordered region, by allowing for partial thermalization of the tunneling electrons. This approach was used by Büttiker[1,2] for the description of zero temperature conductance.

II. FOUR-PROBE THERMOELECTRIC TRANSPORT

Consider the general four-probe system illustrated in Fig. 1. Each probe is a reservoir (characterized by a chemical potential μ_i and a temperature T_i, $i=1,4$) which is connected to a disordered system by a one-dimensional (1D) single-channel perfect lead. It is the connections between the 3D reservoirs and the 1D leads that constitute the contacts. Within linear-response theory[14–17] the net charge and heat currents I_i and Q_i leaving reservoir i can be expressed as

$$I_i=\sum_{j\neq i}\left[\left(\frac{e^2}{h}\right)t_{ij}\,\frac{1}{e}\,(\mu_i-\mu_j)-\left(\frac{\pi^2 e k_B^2 T}{3h}\right)t'_{ij}(T_i-T_j)\right], \tag{1}$$

$$Q_i=\sum_{j\neq i}\left[-\left(\frac{\pi^2 e k_B^2 T^2}{3h}\right)t'_{ij}\,\frac{1}{e}\,(\mu_i-\mu_j)+\left(\frac{\pi^2 k_B^2 T}{3h}\right)t_{ij}(T_i-T_j)\right], \tag{2}$$

which is a generalization of the case of electrical conductance at zero temperature,[1,2] as described in Ref. 3. The

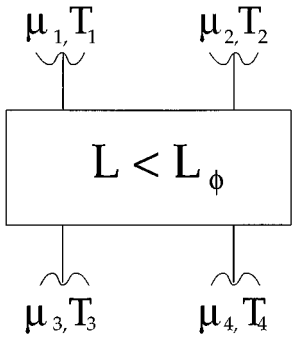

FIG. 1. Schematic illustration of a four-probe setup. Each perfect lead is connected on one side to a reservoir characterized by a chemical potential μ_i and a temperature T_i, $i=1,4$. On the other side the lead is connected to the sample. The linear size of the sample L is less than the dephasing length L_ϕ.

equations were rearranged in order to indicate that the currents are driven by the thermodynamic affinities. The currents are governed by the energy dependent transmission probabilities $t_{ij}(E)$ (note that the notation t_{ij} does not represent an amplitude; also the notation T, without a subscript, denotes the ambient temperature). The coefficient t_{ij} accounts for all interfering paths of an electron in the entire system between contacts i and j while the probes at the remaining contacts are constrained to have the same values of μ and T as the probe i. We assume time-reversal symmetry $t_{ij}(E)=t_{ji}(E)$ and all calculations are done in the Sommerfeld approximation, i.e., the transmission probabilities and their energy derivatives are taken at the Fermi level. In order to demonstrate in a transparent manner the nonlocal nature of the transport coefficients we choose a specific experimental setup. Namely, we allow currents to flow only between probes 1 and 3 and between probes 2 and 4, thereby imposing $I_1=-I_3$, $Q_1=-Q_3$, $I_2=-I_4$, and $Q_2=-Q_4$, due to particle and energy conservation. This is realized experimentally by connecting probes 1–3 and 2–4 with separate charge and heat sources. Note that, since heat is transported only by the electrons, the conditions on the electric currents dictate the same condition on the heat currents. Applying these constraints to Eqs. (1) and (2) enables us to rewrite the equations so that the currents are driven only by the experimental affinities on probes 1–3 and 2–4. These currents will be denoted by I_{13}, I_{24}, Q_{13}, and Q_{24}. Performing the necessary algebra one obtains the matrix form

$$\begin{pmatrix} I_{13} \\ Q_{13} \\ I_{24} \\ Q_{24} \end{pmatrix} = \hat{L}_{4p} \begin{pmatrix} \mu_1/e-\mu_3/e \\ T_1-T_3 \\ \mu_2/e-\mu_4/e \\ T_2-T_4 \end{pmatrix}, \tag{3}$$

where

$$\hat{L}_{4p}=\begin{pmatrix} \sigma_{13,13} & \beta_{13,13} & \alpha_{13,24} & \beta_{13,24} \\ \widetilde{\beta}_{13,13} & \widetilde{\sigma}_{13,13} & \widetilde{\beta}_{13,24} & \widetilde{\alpha}_{13,24} \\ \alpha_{24,13} & \beta_{24,13} & \sigma_{24,24} & \beta_{24,24} \\ \widetilde{\beta}_{24,13} & \widetilde{\alpha}_{24,13} & \widetilde{\beta}_{24,24} & \widetilde{\sigma}_{24,24} \end{pmatrix}. \tag{4}$$

$\hat{L}_{4p}$ is the symmetric four-probe transport matrix in which elements without a tilde represent charge transport coefficients, while those with a tilde represent heat transport coefficients. σ depicts conductance, β is the thermoelectric coupling coefficient, and α is a nonlocal electrical coupling coefficient. The first two indices indicate the probes between which the currents flow, and the latter two indices indicate the probes between which an affinity is applied. Thus $\sigma_{13,13}$ is the Ohmic conductance between probes 1 and 3 and $\widetilde{\beta}_{13,24}$ is the nonlocal thermoelectric coefficient which determines the induced heat current between probes 1 and 3 due to an electric bias between probes 2 and 4. The matrix $\hat{L}_{4p}$ is composed of four (2×2) symmetric submatrices. The diagonal minors include the local transport coefficients, while the off-diagonal minors are nonlocal transport coefficients. The expressions for the coefficients follow.

Top left minor:

$$\sigma_{13,13}=\frac{e^2}{h}\left\{(t_{12}+t_{13}+t_{14})-\frac{t_{12}+t_{14}}{s^2-(\pi^2k_B^2T^2/3)s'^2}\left[s(t_{12}+t_{14})-\frac{\pi^2k_B^2T^2}{3}s'(t'_{21}+t'_{41})\right]\right.$$
$$\left.+\frac{t'_{12}+t'_{14}}{s^2-(\pi^2k_B^2T^2/3)s'^2}\left[\frac{\pi^2k_BT}{3}s'(t_{12}+t_{14})-\frac{\pi^2k_BT}{3}s(t'_{21}+t'_{41})\right]\right\}, \tag{5}$$

$$\beta_{13,13}=\frac{1}{T}\widetilde{\beta}_{13,13}=\frac{ke}{h}\left\{\frac{\pi^2k_BT}{3}(t'_{12}+t'_{13}+t'_{14})-\frac{t_{12}+t_{14}}{s^2-(\pi^2k_B^2T^2/3)s'^2}\left[\frac{\pi^2k_BT}{3}s(t'_{12}+t'_{14})-\frac{\pi^2k_BT}{3}s'(t_{21}+t_{41})\right]\right.$$
$$\left.+\frac{t'_{12}+t'_{14}}{s^2-(\pi^2k_B^2T^2/3)s'^2}\left[\frac{\pi^2k_B^2T^2}{3}s'(t'_{12}+t'_{14})-s(t_{21}+t_{41})\right]\right\}, \tag{6}$$

$$\widetilde{\sigma}_{13,13}=\left(\frac{\pi^2k_B^2T}{3h}\Big/\frac{e^2}{h}\right)\sigma_{13,13}. \tag{7}$$

Top right minor:

$$\alpha_{13,24}=\frac{e^2}{h}\left\{-t_{12}+\frac{t_{12}+t_{14}}{s^2-(\pi^2k_B^2T^2/3)s'^2}\left[s(t_{12}+t_{32})-\frac{\pi^2k_B^2T^2}{3}s'(t'_{21}+t'_{23})\right]-\frac{t'_{12}+t'_{14}}{s^2-(\pi^2k_B^2T^2/3)s'^2}\right.$$
$$\left.\times\left[\frac{\pi^2k_BT}{3}s'(t_{12}+t_{32})-\frac{\pi^2k_BT}{3}s(t'_{21}+t'_{23})\right]\right\}, \tag{8}$$

$$\beta_{13,24}=\frac{1}{T}\widetilde{\beta}_{13,24}=\frac{ke}{h}\left\{-\frac{\pi^2k_BT}{3}t'_{12}+\frac{t_{12}+t_{14}}{s^2-(\pi^2k_B^2T^2/3)s'^2}\left[\frac{\pi^2k_BT}{3}s(t'_{12}+t'_{32})-\frac{\pi^2k_BT}{3}s'(t_{21}+t_{23})\right]\right.$$
$$\left.-\frac{t'_{12}+t'_{14}}{s^2-(\pi^2k_B^2T^2/3)s'^2}\left[\frac{\pi^2k_B^2T^2}{3}s'(t'_{12}+t'_{32})-s(t_{21}+t_{23})\right]\right\}, \tag{9}$$

$$\tilde{\alpha}_{13,24}=\left(\frac{\pi^2 k_B^2 T}{3h}\Big/\frac{e^2}{h}\right)\alpha_{13,24}. \tag{10}$$

Bottom right minor:

$$\sigma_{24,24}=\frac{e^2}{h}\left\{(t_{21}+t_{23}+t_{24})-\frac{t_{12}+t_{23}}{s^2-(\pi^2k_B^2T^2/3)s'^2}\left[s(t_{21}+t_{23})-\frac{\pi^2k_B^2T^2}{3}s'(t'_{12}+t'_{32})\right]+\frac{t'_{12}+t'_{23}}{s^2-(\pi^2k_B^2T^2/3)s'^2}\right.$$
$$\left.\times\left[\frac{\pi^2k_BT}{3}s'(t_{12}+t_{23})-\frac{\pi^2k_BT}{3}s(t'_{12}+t'_{32})\right]\right\}, \tag{11}$$

$$\beta_{24,24}=\frac{1}{T}\tilde{\beta}_{24,24}=\frac{ke}{h}\left\{\frac{\pi^2k_BT}{3}(t'_{21}+t'_{23}+t'_{24})-\frac{t_{12}+t_{23}}{s^2-(\pi^2k_B^2T^2/3)s'^2}\left[\frac{\pi^2k_BT}{3}s(t'_{21}+t'_{23})-\frac{\pi^2k_BT}{3}s'(t_{12}+t_{32})\right]\right.$$
$$\left.+\frac{t'_{12}+t'_{23}}{s^2-(\pi^2k_B^2T^2/3)s'^2}\left[\frac{\pi^2k_B^2T^2}{3}s'(t'_{21}+t'_{23})-s(t_{12}+t_{32})\right]\right\}, \tag{12}$$

$$\tilde{\sigma}_{24,24}=\left(\frac{\pi^2k_B^2T}{3h}\Big/\frac{e^2}{h}\right)\sigma_{24,24}. \tag{13}$$

Bottom left minor:

$$\alpha_{24,13}=\alpha_{13,24}, \tag{14}$$

$$\beta_{24,13}=\tilde{\beta}_{24,13}=\beta_{13,24}=\tilde{\beta}_{13,24}, \tag{15}$$

$$\tilde{\alpha}_{24,13}=\left(\frac{\pi^2k_B^2T}{3h}\Big/\frac{e^2}{h}\right)\alpha_{24,13}, \tag{16}$$

where

$$s=t_{12}+t_{14}+t_{32}+t_{34}. \tag{17}$$

We note that the Onsager reciprocity relations are satisfied and that the nonlocal coupling terms $\alpha_{ij,kl}$ generalize some zero temperature results. Indeed, when the zero temperature limit is taken in Eqs. (5)–(16) the $T=0$ results are recovered.[1,2] The symmetry relations ensue from the time-reversal invariance of the transmission coefficients. In the case of an external magnetic field B threading the mesoscopic region, the relations $t_{ij}(B)=t_{ji}(-B)$ ensure that the symmetry of the transport matrix in Eq. (4) is maintained, provided the magnetic field is reversed in addition to the time reversal, i.e.,

$$\hat{L}(B)=\hat{L}^{\dagger}(-B), \tag{18}$$

where the dagger denotes the transposed matrix [and when properly accounting for inverse temperature as in Eq. (6)].

One can use Eqs. (5)–(16) to define nonlocal thermopower. For example,

$$S_{13,24}\equiv-\left.\frac{V_1-V_3}{T_2-T_4}\right|_{I_{13}=0,V_2=V_4,T_1=T_3}=-\frac{\beta_{13,24}}{\sigma_{13,13}}, \tag{19}$$

where $V_i\equiv\mu_i/e$. However, as noted in Ref. 3, the nonlocal thermopower is not symmetric with respect to interchanging the roles of the voltage and current probes, i.e., $S_{ij,kl}(B)\neq S_{kl,ij}(-B)$. This follows from the dependence of the conductance σ on the specific probes sustaining the transport. For example, $S_{13,24}(B)\neq S_{24,13}(-B)$ since $\sigma_{13,13}\neq\sigma_{24,24}$. Another result of the definition Eq. (19) is that the thermoelectric coefficients are generally asymmetric in magnetic field, i.e., $S_{ij,kl}(B)\neq S_{ij,kl}(-B)$, due to the asymmetry of the transmission $t_{ij}(B)$. This is a generalization of asymmetric magnetoconductance, which is measured in four-probe devices, as discussed in Ref. 1.

III. THE LIMIT OF TWO PROBES

The above formalism can be exploited to determine the transport coefficients of a mesoscopic region (disregarding the contact contribution) for a two-probe configuration. We implement the Engquist-Anderson[2,9] picture by examining the setup in Fig. 2, which describes a $1D$ single-channel system. Adopting the approach of Landauer,[18] we represent the region of disordered elastic scatters by an effective elastic scattering barrier, characterized by transmission and reflection coefficients t and r, respectively. Probes 2 and 4 are used to measure the induced thermodynamic potentials which develop as a result of transport between reservoirs 1 and 3. Therefore we require

$$I_{24}=Q_{24}=0, \tag{20}$$

corresponding to infinite resistance of ideal measuring devices. This measurement is performed in the limit of *weak coupling* of the probes to the mesoscopic sample. The reservoirs are connected to the disordered region (described by a single barrier) by perfect leads and an S matrix. Weak coupling is incorporated into the equations by assigning a coupling of order $\epsilon\to 0$ to leads 2 and 4. The (3×3) scattering matrices are chosen as in Ref. 19. Namely, time-reversal symmetry and particle conservation are satisfied. We assume the S matrices allow symmetric scattering into the two branches leading out of reservoirs 2 and 4, and that the matrix is real. The latter assumption guarantees that contacts 2

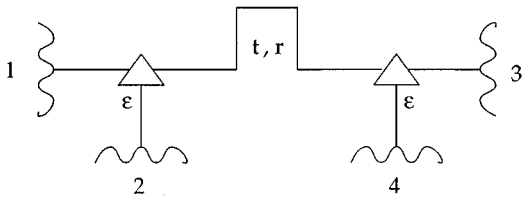

FIG. 2. A specific four-probe configuration in which probes 1 and 3 are strongly coupled to leads to the disordered region. Probes 2 and 4 are variably coupled with a coupling strength ϵ. The triangles represent a three-sided junction characterized by two symmetric (3×3) S matrices (see text). The barrier is characterized by a (2×2) matrix, the elements of which are the transmission and reflection coefficients t and r, respectively.

and 4 do not alter the phase of the traversing electron so that in the limit $\epsilon\rightarrow 0$ the system is reduced to a two-probe setup. Such an S matrix has the form

$$\hat{S}=\begin{pmatrix} c & \sqrt{\epsilon/2} & \sqrt{\epsilon/2} \\ \sqrt{\epsilon/2} & a & b \\ \sqrt{\epsilon/2} & b & a \end{pmatrix} \tag{21}$$

satisfying $\vec{\alpha}=\hat{S}\vec{\beta}$. $\vec{\alpha}=(\alpha_1,\alpha_2,\alpha_3)$ are the outgoing amplitudes where α_1 is the amplitude of an electron wave function leaving the junction (triangles in Fig. 2) towards reservoir 2 (4). The amplitudes to leave the junction in the direction of reservoirs 1 and 3 are denoted by α_2 and α_3, respectively. The ingoing amplitudes are denoted by β_i. In order to ensure the unitarity property of $\hat{S}$, we choose a, b, and c to be

$$a=\frac{1}{2}\,(\sqrt{1-\epsilon}-1), \tag{22}$$

$$b=\frac{1}{2}\,(\sqrt{1-\epsilon}+1), \tag{23}$$

$$c=-\sqrt{1-\epsilon}, \tag{24}$$

where $0\leqslant\epsilon\leqslant 1$. The transport in Fig. 2 is determined by the scattering amplitudes of an electron along its path, which is given by three S matrices: two [like Eq. (21)] at contacts 2 and 4, and another one at the barrier. The barrier transmission and reflection probabilities (not amplitudes) are denoted by t and r, respectively, and represent the elastic scattering in the mesoscopic region. We assume that quantum oscillations in the interference pattern of the reflected electron can be neglected. This assumption corresponds to measuring devices (i.e., the contacts) with a linear size W of several Fermi wavelengths λ_F, thereby effectively averaging (spatially) over the phase of an electron (at the Fermi level). This assumption is valid for $\lambda_F/(\pi W)\ll\sqrt{|r|}$. In very disordered systems $\sqrt{|r|}\rightarrow 1$. Accounting for single-scattering processes (multiple scattering can be neglected in the weak-coupling limit), one obtains the following transmission coefficients: $t_{13}=t$, $t_{24}=t(\epsilon/2)^2$, $t_{14}=t_{23}=t\epsilon/2$, $t_{12}=t_{34}=(1+r)\epsilon/2$ and, in turn, $s=2\epsilon$ and $s'=0$. Inserting these transmission coefficients into Eqs. (3)–(17) we obtain

$$I_{24}=-\frac{e^2}{h}\,r\,\frac{\epsilon}{2}\,\frac{1}{e}\,(\mu_1-\mu_3)+\frac{e^2}{h}\left(1+t\,\frac{\epsilon}{2}\right)\frac{\epsilon}{2}\,\frac{1}{e}\,(\mu_2-\mu_4) - \frac{e\pi^2k_B^2T}{3h}\,t'\,\frac{\epsilon}{2}\,(T_1-T_3)-\frac{e\pi^2k_B^2T}{3h}\,t'\left(\frac{\epsilon}{2}\right)^2(T_2-T_4), \tag{25}$$

$$Q_{24}=-\frac{e\pi^2k_B^2T^2}{3h}\,t'\,\frac{\epsilon}{2}\,\frac{1}{e}\,(\mu_1-\mu_3) - \frac{e\pi^2k_B^2T^2}{3h}\,t'\left(\frac{\epsilon}{2}\right)^2\frac{1}{e}\,(\mu_2-\mu_4)-\frac{\pi^2k_B^2T}{3h}\,r\,\frac{\epsilon}{2} \times(T_1-T_3)+\frac{\pi^2k_B^2T}{3h}\left(1+t\,\frac{\epsilon}{2}\right)\frac{\epsilon}{2}\,(T_2-T_4). \tag{26}$$

Using Eqs. (25) and (26), we can rewrite the condition Eq. (20) in a matrix form in the following way:

$$\hat{A}\begin{pmatrix}\mu_1/e-\mu_3/e\\ T_1-T_3\end{pmatrix}=\hat{B}\begin{pmatrix}\mu_2/e-\mu_4/e\\ T_2-T_4\end{pmatrix}, \tag{27}$$

where

$$\hat{A}=\begin{pmatrix} -\dfrac{e^2}{h}\,r & -\dfrac{e\pi^2k_B^2T}{3h}\,t' \\ -\dfrac{e\pi^2k_B^2T^2}{3h}\,t' & -\dfrac{\pi^2k_B^2T}{3h}\,r \end{pmatrix} \tag{28}$$

and

$$\hat{B}=\begin{pmatrix} -\dfrac{e^2}{h}\left(1+t\,\dfrac{\epsilon}{2}\right) & \dfrac{e\pi^2k_B^2T}{3h}\,t'\,\dfrac{\epsilon}{2} \\ \dfrac{e\pi^2k_B^2T^2}{3h}\,t'\,\dfrac{\epsilon}{2} & -\dfrac{\pi^2k_B^2T}{3h}\left(1+t\,\dfrac{\epsilon}{2}\right) \end{pmatrix}. \tag{29}$$

We take the limit $\epsilon\rightarrow 0$ and, as expected, the currents I_{13} and Q_{13} become independent of $(\mu_2-\mu_4)$ and (T_2-T_4). Equation (3) then reduces to the familiar two-probe form

$$\begin{pmatrix}I_{13}\\ Q_{13}\end{pmatrix}=\hat{L}_{2p}\begin{pmatrix}\mu_1/e-\mu_3/e\\ T_1-T_3\end{pmatrix}, \tag{30}$$

where

$$\hat{L}_{2p}=\begin{pmatrix} \dfrac{e^2}{h}\,t & -\dfrac{e\pi^2k_B^2T}{3h}\,t' \\ -\dfrac{e\pi^2k_B^2T^2}{3h}\,t' & \dfrac{\pi^2k_B^2T}{3h}\,t \end{pmatrix}. \tag{31}$$

Combining Eqs. (27) and (30) we can write

$$\begin{pmatrix}I_{13}\\ Q_{13}\end{pmatrix}=\hat{L}_{2p}\hat{A}^{-1}\hat{B}\begin{pmatrix}\mu_2/e-\mu_4/e\\ T_2-T_4\end{pmatrix}, \tag{32}$$

which relates the affinity developed across the barrier to the currents driven between probes 1 and 3. The matrix

$$\hat{K}\equiv\hat{L}_{2p}\hat{A}^{-1}\hat{B} \tag{33}$$

defines the transport coefficients of the barrier in the interpretation of Ref. 9. Inserting Eqs. (28), (29), and (31) into Eq. (33) yields the coefficients

$$K_{11}=\frac{\frac{e^2}{h}\left[rt+\frac{\pi^2}{3}(k_BT)^2t'^2\right]}{r^2-\frac{\pi^2}{3}(k_BT)^2t'^2}, \tag{34}$$

$$K_{12}=-\frac{\frac{k_Be}{h}\frac{\pi^2}{3}(k_BT)t'}{r^2-\frac{\pi^2}{3}(k_BT)^2t'^2}, \tag{35}$$

$$K_{21}=TK_{12}, \tag{36}$$

$$K_{22}=\frac{\frac{\pi^2}{3}\frac{k_B^2T}{h}\left[rt+\frac{\pi^2}{3}(k_BT)^2t'^2\right]}{r^2-\frac{\pi^2}{3}(k_BT)^2t'^2}. \tag{37}$$

Note that $\hat{K}$ satisfies the Onsager relation [Eq. (36)]. Neglecting terms including $(k_BT)^2t'^2$ with respect to terms including r,t we obtain

$$K_{11}=\frac{e^2}{h}\frac{t}{r}, \tag{38}$$

$$K_{21}=TK_{12}=-\frac{\pi^2}{3}\frac{(k_BT)^2e}{h}\left(\frac{t}{r}\right)', \tag{39}$$

$$K_{22}=\frac{\pi^2}{3}\frac{k_B^2T}{h}\frac{t}{r}. \tag{40}$$

Equations (38)–(40) are identical to the expressions obtained in Ref. 13. In that paper these coefficients were obtained for a two-probe system in similar limits. Namely, it was assumed that the Sommerfeld approximation is valid. In addition, $(k_BT)^2t'^2$ terms were neglected with respect to terms quadratic in r,t. Comparing Eqs. (38)–(40) to the results of Ref. 12, we find that the expressions for K_{11}, K_{12}, and K_{22} are identical in the Sommerfeld approximation. However, in that paper the Onsager relations were not satisfied for the mesoscopic region, since it was found that $K_{21}=TK_{12}+\text{const}$. In our theory, those relations are satisfied. We believe this happened because we were careful to ascribe thermodynamic properties and parameters (e.g., temperature, chemical potential) only to equilibrium physical systems, such as a macroscopic probe, and not to parts of the mesoscopic physical system.

The thermopower of the barrier is defined as

$$S_b\equiv-\frac{K_{12}}{K_{11}}$$

and in the above limits this becomes

$$S_b=\frac{\pi^2}{3}\frac{k_B^2T}{e}\left(\ln\frac{t}{1-t}\right)', \tag{41}$$

as we obtained in Refs. 12 and 13.

IV. THE EFFECT OF INCOHERENT TRANSPORT

The simplified system analyzed in Sec. III can be used to demonstrate the effect of partial phase incoherence on the transport. This is seen by calculating the transport coefficients in the limit of strong coupling, i.e., $\epsilon\to1$. Electrons driven between probes 1 and 3 have a probability of 1/2 to enter the reservoirs at each of the contacts 2 and 4, due to our choice of the S matrix in Eq. (21). The electron waves entering reservoirs 2 and 4 thermalize and lose phase coherence. Since probes 2 and 4 are measurement contacts, $I_{24}=Q_{24}=0$. This ensures that the thermalized part is reinjected into the system and recombines with the wave that proceeded ballistically. Thus electrons traversing the sample lose partial phase coherence. As before, we neglect quantum oscillations and multiple scattering. The transmission coefficients corresponding to Fig. 2 are obtained as before in terms of the scattering matrix elements to give $t_{13}=t_{24}=t/4$, $t_{14}=t_{23}=t/8$, $t_{12}=t_{34}=(1/2+r/8)$ and, in turn, $s=5/4$ and $s'=0$. The partial loss of phase coherence is reflected in coefficients $t_{14}=t_{23}$ and $t_{12}=t_{34}$ which do not include the amplitude of an electron injected from reservoirs 2 and 4. Inserting the coefficients into Eqs. (3), the currents driven between probes 1 and 3 become

$$I_{13}=\frac{e^2}{h}\left(\frac{t}{4}+\frac{5}{16}\right)\frac{1}{e}(\mu_1-\mu_3)-\frac{e^2}{h}\left(\frac{r}{8}+\frac{3}{16}\right)\frac{1}{e}(\mu_2-\mu_4)$$
$$-\frac{e\pi^2k_B^2T}{3h}\frac{t'}{4}(T_1-T_3)-\frac{e\pi^2k_B^2T}{3h}\frac{t'}{8}(T_2-T_4), \tag{42}$$

$$Q_{13}=-\frac{e\pi^2k_B^2T^2}{3h}\frac{t'}{4}\frac{1}{e}(\mu_1-\mu_3)-\frac{e\pi^2k_B^2T^2}{3h}\frac{t'}{8}\frac{1}{e}$$
$$\times(\mu_2-\mu_4)+\frac{\pi^2k_B^2T}{3h}\left(\frac{t}{4}+\frac{5}{16}\right)(T_1-T_3)$$
$$-\frac{\pi^2k_B^2T}{3h}\left(\frac{r}{8}+\frac{3}{16}\right)(T_2-T_4). \tag{43}$$

Rewriting Eqs. (27)–(29) in the limit $\epsilon=1$, we can express I_{13} and Q_{13} as a function of the affinity between probes 1 and 3. Neglecting, for simplicity, $(k_BT)^2t'^2$ terms, we obtain [see Eq. (30)]

$$L_{11}^{\epsilon=1}=\frac{75+75t+12t^2}{100+160t+64t^2}L_{11}^{\epsilon=0}, \tag{44}$$

$$L_{21}^{\epsilon=1}=TL_{12}^{\epsilon=1}=\frac{75+30t+12t^2}{100+160t+64t^2}L_{12}^{\epsilon=0}, \tag{45}$$

$$L_{22}^{\epsilon=1}=\frac{75+75t+12t^2}{100+160t+64t^2}L_{22}^{\epsilon=0}. \tag{46}$$

The coefficients L_{ij} represent the measurable transport between probes 1 and 3, i.e., they include the contribution of the contacts. $L_{ij}^{\epsilon=0}$ denotes the two-probe matrix element in Eq. (31). In Fig. 3 we plot the ratio $L_{11}^{\epsilon=1}/L_{11}^{\epsilon=0}\equiv G^{\epsilon=1}/G^{\epsilon=0}$ as a function of the barrier transmission t. Note that in

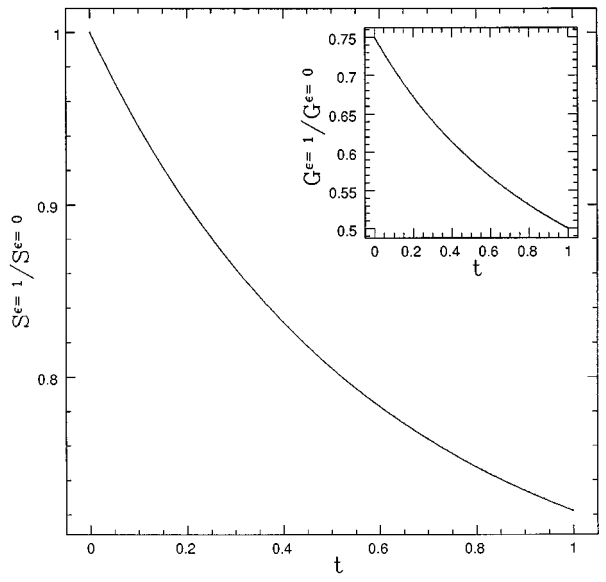

FIG. 3. A numerical calculation of Eq. (47) demonstrating the effect of partial dephasing in reservoirs 2 and 4 on the two-probe thermopower of the system of Fig. 2. The inset demonstrates the effect on the electrical conductance [Eq. (44)].

addition to loss of phase coherence the splitters at reservoirs 2 and 4 partially reflect the incident electron wave function. This is a result of our choice of S matrices which are constrained to ensure perfect transmission in the limit $\epsilon \to 0$. The combined effect is to reduce the electrical and heat conductances.

The thermopower $S = -L_{12}/L_{11}$ in the strong-coupling limit satisfies the relation

$$S^{\epsilon=1} = \frac{25+10t+4t^2}{25+25t+4t^2}\, S^{\epsilon=0}. \tag{47}$$

The partial loss of phase coherence and splitter reflection act to lower the thermopower, as illustrated in Fig. 3. The reduction of conductance $G^{\epsilon=1}$ and thermopower $S^{\epsilon=1}$, compared to the weak-coupling limit, is enhanced as $t \to 1$. This could be attributed to the dephasing mechanism becoming more dominant, as more of the electron wave traverses the barrier. Note that the results of this section are valid only when multiple scattering between the barrier and contacts 2 and 4 can be neglected. We expect the correction due to this effect to be largest in the limit of $t \to 1$ and $t \to 0$.

V. CONCLUSION

In this paper we considered specific configurations of multiprobe systems in which one can define a nonlocal thermoelectric response. It should be possible to realize such a system experimentally. In particular, we expect that the effect of partial phase incoherence in a system like the one in Fig. 2 can be measured. Reservoirs 2 and 4 represent point-contact measurement probes. Tuning the distance between the point contacts and the sample, one can realize the limits $\epsilon \to 0$ and $\epsilon = 1$ and measure the transport through a disordered region between fixed probes (realizing probes 1 and 3). In order to justify the neglect of quantum oscillations the contacts must be several Fermi wavelengths wide. The transmission t can be obtained from the two-probe conductance measurement ($\epsilon = 0$). Note that in order to compare to theoretical predictions the structure of the S matrix might need adjustment in order to correctly represent the experimental setup. In future work we will study the explicit effect of total phase incoherence across the sample by choosing nonreflecting S matrices for the splitters.

An experimental realization of a four-probe system is predicted to exhibit nonlocal thermopower [Eq. (19)]. Heating probes 1 and 3 will produce a measurable temperature gradient and will induce an electric potential drop between the other two terminals.

In the above analysis we neglected quantum oscillations resulting from electron interference at the measurement probes 2 and 4. We also disregarded multiple-scattering processes in the mesoscopic region. These processes are relevant in the strong-coupling limit and can be incorporated in the model, yielding corrections to the above results. An exact quantum-mechanical treatment has been given for similar systems in Refs. 20 and 21 in the case of zero temperature. As a result one obtains phase-sensitive Ohmic voltages which depend on the distance of these probes from the scatterer. By expanding the work reported here, we expect to obtain phase-sensitive thermoelectric voltages which can be measured using point-contact probes.

The calculations in this paper were performed in the Sommerfeld approximation. Therefore the results are valid in the case that the transmission coefficients depend smoothly on energy. Equations (38)–(41) and (44)–(47) are valid when terms including $(k_B T)^2 t'^2$ are disregarded with respect to terms quadratic in t and r. This approximation is usually accurate for the following reason. In Ref. 22 the quantity

$$\Delta \equiv \frac{\mathbf{L}_{12}\mathbf{L}_{21}}{\mathbf{L}_{11}\mathbf{L}_{22}} \tag{48}$$

was defined for a two-probe system. Δ is related to the efficiency of the thermoelectric effect and in many cases satisfies $\Delta \ll 1$. It is easy to show that in the Sommerfeld approximation

$$\Delta = \frac{\pi^2}{3}\,(k_B T)^2 \left(\frac{t'}{t}\right)^2,$$

thereby ensuring that if $\Delta \ll 1$ the condition $(k_B T t')^2 \ll t^2$ is satisfied.

ACKNOWLEDGMENTS

Partial support for this work was provided by the Israel Science Foundation, Grant Number 593/95, and the US-Israel Binational Science Foundation.

[1] M. Büttiker, Phys. Rev. Lett. **57**, 1761 (1986).
[2] M. Büttiker, IBM J. Res. Dev. **32**, 317 (1988).
[3] P. N. Butcher, J. Phys. Condens. Matter **2**, 4869 (1990).
[4] M. Ya. Azbel, Phys. Rev. B **47**, 15 688 (1993).
[5] R. Landauer, Philos. Mag. **21**, 863 (1970).
[6] Y. Imry, *Directions in Condensed Matter Physics* (World Scientific Press, Singapore, 1986).
[7] E. N. Economou and C. M. Soukoulis, Phys. Rev. Lett. **46**, 618 (1981).
[8] A. D. Stone and A. Szafer, IBM J. Res. Dev. **32**, 384 (1988).
[9] H. L. Engquist and P. W. Anderson, Phys. Rev. B **24**, 1151 (1981).
[10] M. Ya. Azbel, J. Phys. C **14**, L225 (1981).
[11] M. Büttiker, Y. Imry, R. Landauer, and S. Pinhas, Phys. Rev. B **31**, 6207 (1985).
[12] U. Sivan and Y. Imry, Phys. Rev. B **33**, 551 (1986).
[13] G. D. Gutmann, E. Ben-Jacob, and D. J. Bergman, Phys. Rev. B **52**, 5256 (1995).
[14] G. V. Chester and A. Thellung, Proc. Phys. Soc. London **77**, 1005 (1961).
[15] M. J. Kearney and P. N. Butcher, J. Phys. C **21**, L265 (1988).
[16] C. Castellani, C. Di Castro, M. Grilli, and G. Strinati, Phys. Rev. B **37**, 6663 (1988).
[17] G. D. Guttman, E. Ben-Jacob, and D. J. Bergman, Phys. Rev. B **51**, 17 758 (1995).
[18] R. Landauer, IBM J. Res. Dev. **1**, 223 (1957).
[19] M. Büttiker, Y. Imry, and M. Ya. Azbel, Phys. Rev. A **30**, 1982 (1984).
[20] M. Büttiker, Phys. Rev. B **40**, 3409 (1989).
[21] M. Büttiker, IBM J. Res. Dev. **32**, 63 (1988).
[22] D. J. Bergman and O. Levy, J. Appl. Phys. **70**, 6821 (1991).